A Simplified and Cost-Effective Fiber Laser Fabrication Method for Designing Wideband Multi-Layer Fabry-Perot/Leaky-Wave Antenna with Complementary PRS

Rana Muhammad Hasan Bilal(1), Etienne Perret(2),(3), Simone Genovesi(1), Giuliano Manara(1), and Filippo Costa(1)
(1) Department of Information Engineering, University of Pisa, 56125 Pisa, Italy.
(2) Univ. Grenoble Alpes, Grenoble INP, LCIS, 26000 Valence, France.
(3) Institut Universitaire de France, 75005 Paris, France.

Abstract

In this article, we present a simplified, fast, cost-effective, and precise fabrication method for designing multi-layer leaky-wave/Fabry-Perot antennas (LWAs/FPAs). Traditionally, these antennas are fabricated using existing techniques such as lithography, LPKF laser, and 3D printing. The proposed antenna design features a pair of complementary partially reflective surfaces (PRSs) printed on either side of a low-cost plastic substrate. This substrate is positioned over an air cavity backed by a metallic ground plane, which includes a slot to accommodate waveguide feeding. The proposed FPA achieves a high gain of approximately 14 dBi across a wide operating frequency range (20-21.86 GHz), with excellent impedance matching characterized by an S_{11} level below -10 dB. The antenna is fabricated using a fiber laser fabrication method, which is a simple, efficient, and fast process, taking less than a minute to create the periodic patterns for the desired samples. Finally, its simulation results are validated through multiple measurements conducted on various samples.

1 Introduction

High gain antennas are very important and crucial components for the applications including satellite communication [1], radar detection [2], air traffic control [3], astronomy [4] and millimeter-wave (mm-wave) communication [5]. Conventionally, antenna arrays are designed to achieve increased gain by combining the radiated energy from multiple individual antennas [6]. These antennas are arranged in a specific configuration and excited simultaneously with controlled amplitude and phase to produce a focused and directive beam, resulting in high gain. Although these specific antennas can achieve high gain, their feeding mechanisms, such as corporate feeding networks [7], Butler matrices [8], and others, are inherently complex and challenging to implement.

Alternatively, FPAs provide high gain but have a narrow bandwidth [9, 10]. They offer a simplified design geometry and straightforward feeding mechanism, making them a potential replacement for conventional antenna arrays [9, 10]. They have proven to be an effective solution for high directive applications because of their simple and easily fabricable design, which incorporates an air cavity positioned at half the wavelength between the ground plane and the top PRS [11]. The most significant and straightforward aspect of these antennas is their excitation, as they can be easily fed using a simple waveguide source, eliminating the need for a complex feeding network typically required in multiple-input multiple-output (MIMO) antenna arrays [10, 11]. In the past, various design approaches for implementing FP antennas have been studied and include dielectric superstrates [12], electromagnetic band-gap structures [13], multiple-layer PRS [14, 15] and single-layer PRS [16, 17] etc.

Currently, wideband FPAs are in great demand. Their bandwidth can be enhanced through various design strategies, such as using complementary PRS [14, 15], multi-fed excitation [11, 18], or a combination of these approaches. In a complementary PRS-based approach, one or two complementary PRS are placed above the air cavity to achieve a positive phase gradient within the desired operating frequency range, thereby enhancing the bandwidth. Similarly, in the multi-fed method, multiple excitation sources are strategically employed to stimulate the cavity at different points, effectively broadening the operating bandwidth.

In this article, a wideband FPA is designed and fabricated using a simple, efficient, and cost-effective method involving a fiber laser marker machine. The proposed antenna employs a positive phase gradient approach, achieved through the implementation of a complementary PRS periodic array within the desired operational band. The FPA demonstrates wideband performance, achieving a 3 dB gain of 14 dBi and maintaining an S_{11} level below -10 dB across the operating frequency range. The proposed fiber laser method enables the eco-friendly fabrication of precise, low-cost FSS devices in under a minute, without hazardous chemicals.

2 Design of the Complementary PRS-Based FPA

The standard configuration of an FPA typically consists of a single PRS separated from the ground plane by an air spacer, which results in narrowband characteristics. The proposed antenna layout, however, adopts a multilayer design to achieve a wideband response. It features a periodic array of square patches printed on the top surface of a plastic substrate ($\varepsilon_r = 2.5$, $\tan\delta = 0.03$), while the backside of the substrate is patterned with periodic grid elements, serving as the PRS. This PRS is separated from the ground plane by an air-filled cavity of height h_0, which forms the resonant cavity of the antenna. The proposed FPA is excited using a rectangular waveguide (WR42) positioned beneath

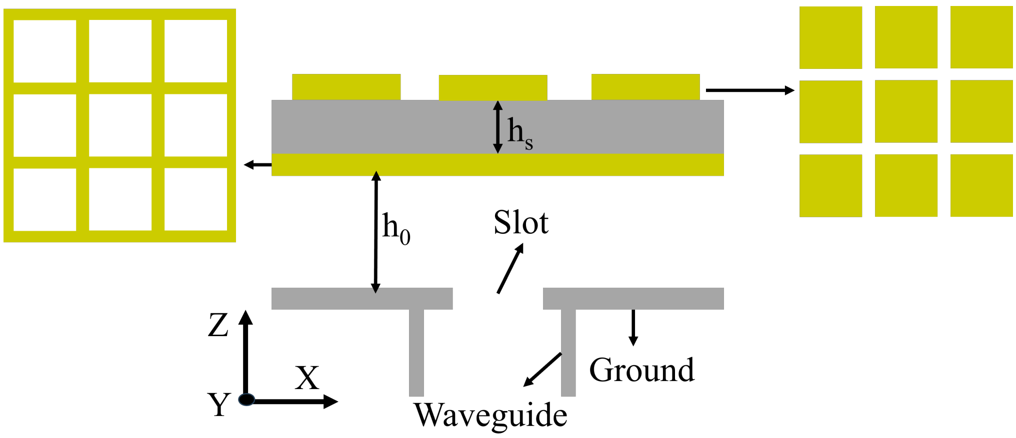

Figure 1. Schematic representation of the proposed FPA, featuring a complementary PRS composed of a periodic array of square patches and grid elements printed on opposite sides of a plastic substrate. The substrate is positioned at a distance of h_0 from the bottom ground plane, which includes a feeding slot to accommodate the rectangular waveguide for excitation.

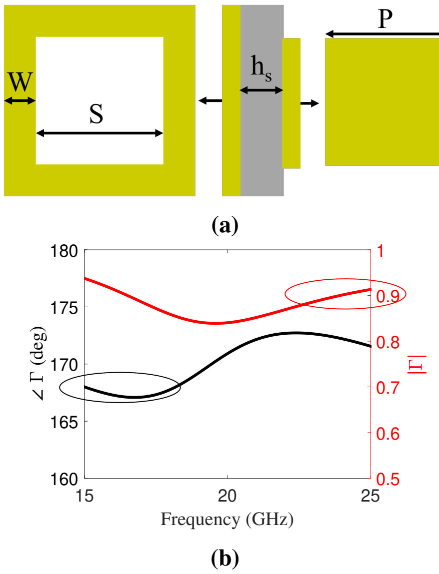

Figure 2. (a) Side view of the PRS unit cell, featuring a square patch on one side and a grid on the opposite side of the plastic substrate with P = 3 mm, S = 3 mm and W = 1 mm and h_s = 1 mm, (b) Reflection features of the unit cell of the designed PRS.

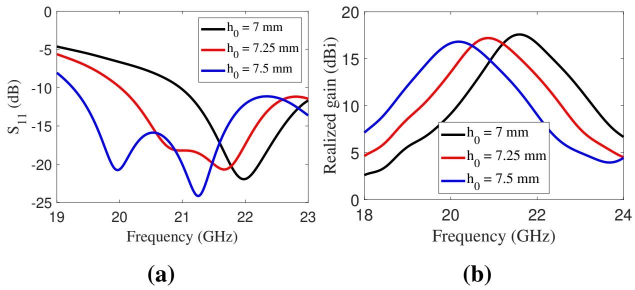

Figure 3. Performance analysis of the proposed FPA with varying height (h_0) of the air cavity: (a) Reflection coefficient (S_{11}) trends indicating good impedance matching, and (b) Gain trends highlighting the influence of air cavity height on antenna radiation performance.

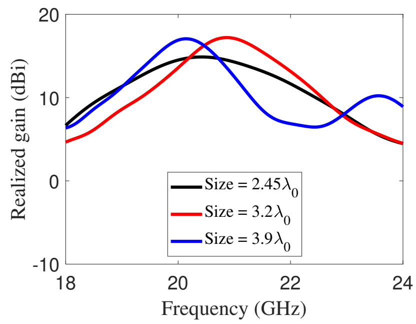

Figure 4. Gain variation of the proposed FPA for different antenna sizes, where λ_0 represents the wavelength corresponding to the operating frequency (f_0) of 21 GHz.

the slotted ground plane. The complete configuration of the FPA is depicted in Fig. 1. The design and simulation of the antenna structure are carried out using CST Studio Suite, utilizing its built-in time-domain solver.

3 Results and Discussion

To design a wideband Fabry-Perot antenna (FPA), the positive phase gradient method is employed. It utilizes a complementary PRS to achieve positive phase progression within the desired operating frequency range. The unit cell of a PRS consists of a square patch printed on one side of the plastic substrate, while grid element is printed on the opposite side, as illustrated in Fig. 2a. The effective design parameters of the unit cell, including the periodicity (D),

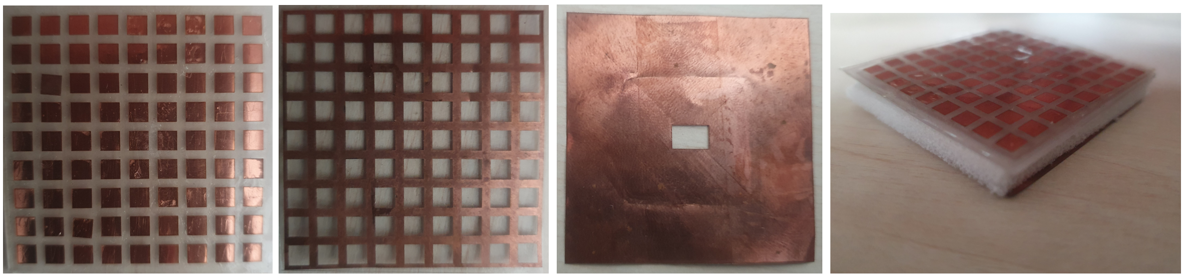

(a) (b) (c) (d)

Figure 5. Fabrication section of the proposed FPA, showing layer by layer component, (a) Periodic array of the square patches (b) Periodic array of the grids, (c) Bottom ground plane includes a slot designed to accommodate the waveguide feeding and (d) The complete antenna structure is composed of multiple layers arranged as follows: the top layer is a plastic tape, followed by a second layer of periodic array of copper patches. The third layer consists of a plastic substrate, while the fourth layer features a periodic array of grids. The fifth layer comprises foam, utilized to form the air cavity, and the sixth layer serves as the bottom ground plane.

patch size (P), slot size (S), grid width (W), and dielectric thickness (h_s), are optimized to achieve the desired positive phase response within the targeted frequency band. Their optimized values are as follows: D = 5 mm, P = 3 mm, S = 3 mm, W = 1 mm and h_s = 1 mm. The corresponding reflection amplitude and phase of the PRS are shown in Fig. 2b, revealing that the phase gradient becomes positive at 18 GHz and maintains a positive slope up to 21 GHz. This indicates that the FPA can achieve a broad bandwidth within this frequency range.

Now, to obtain the wideband characteristics of an FPA, the complete antenna layout is designed with an overall size of of 45 mm $\times$ 45 mm, comprising an array of 9×9 unit cells of patches and grid elements. The air-spacer cavity height (h_0) is optimized to be 7.25 mm which is $\lambda_0/2$ at the operating frequency of 21 GHz. The proposed FPA is excited through a rectangular waveguide feeding mechanism owing to its simple and straightforward feeding. The length and width of the grounded slot are 8.5 mm and 4.25 mm respectively. The simulated realized gain and S_{11} are shown in Fig. 3 for varying h_0. The results indicate that the FPA achieves good impedance matching across a wide operating frequency band, with a high peak gain of 17.2 dBi and an overall gain of 14 dBi within the operational frequency spectrum. The gain characteristics of the proposed antenna are analyzed for various antenna sizes, as shown in Fig. 4. It is observed that the antenna with a size of $3.2\lambda_0$ achieves high gain over a wide operating bandwidth, outperforming other antenna sizes.

4 Fabrication and Measurements

This section describes the fabrication process for the FPA, which consists of a pair of complementary PRS. A 9×9 array of square patches, with a total sample size of 45 mm $\times$ 45 mm, is cut using a fiber laser marking machine, as presented in Fig. 5a. This process is completed in under a minute, demonstrating its speed and time-saving efficiency. During the cutting, the remaining mask forms a periodic array of grid elements, as seen in Fig. 5b. Since the patches and grids are exact complements of each other, there is no

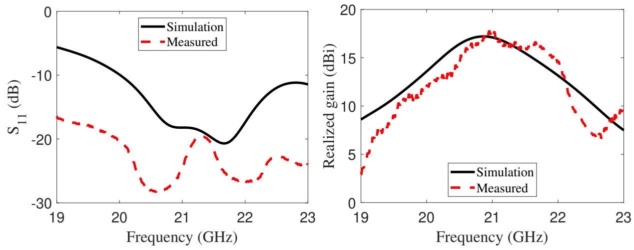

(a) (b)

Figure 6. Comparison of the full-wave Simulation and measured (a) S_{11} (b) realized gain of the FPA. Measurements are conducted on two different prototypes to verify the replicability of results and fabrication tolerances.

need to prepare the grid elements separately.

A 45 mm $\times$ 45 mm copper patch is then prepared, and a slot is made using the fiber laser machine to accommodate the waveguide for antenna feeding. This slotted square patch serves as a bottom ground-plane, as shown in Fig. 5c. The square patches are collected using standard scotch tape and transferred onto one side of a plastic substrate, while the remaining grid array is transferred onto the other side. To create the air cavity, a foam layer with an approximately thickness of 7 mm is used. Finally, the plastic substrate with patches and grid elements is positioned over the foam, with the slotted ground plane placed at the bottom side of the foam. This method efficiently fabricates the FPA structure with complementary PRS elements and the entire antenna is presented in 5d.

To evaluate the performance of the fabricated FPA, the prototype was connected to a vector network analyzer (VNA) and fed using a rectangular waveguide (WR42) to excite the antenna. The measured S_{11} parameter was obtained and compared with the simulated results, as shown in Fig. 6a. Both the simulated and measured S_{11} exhibit values below -10 dB over a wide operating frequency range. Although both curves display two resonance dips, discrepancies are observed between them. These discrepancies are attributed to improper tightening and misalignment of the waveguide with the bottom slotted ground plane. As shown in Fig. 5c, the back side of the FPA, which consists of the slotted ground plane, lacks alignment holes to properly secure the waveguide. This misalignment leads to inconsistencies between the simulated and measured S_{11} parameters. Additionally, the simulated and measured gain curves show good agreement, as presented in Fig. 6b.

5 Conclusion

This paper demonstrated a design and fabrication of a low-cost, wideband multi-layer FPA with a complementary PRS approach. The proposed FPA utilized a pair of complementary PRS structures on either side of the low-cost plastic substrate, which provided a positive phase gradient, thereby enhancing the antenna bandwidth. The antenna demonstrated a wide bandwidth ranging from 20 GHz to 21.86 GHz with a 3 dB gain of 14 dBi and excellent impedance matching. The step-by-step fabrication process was given and the antenna was manufactured using a fast and efficient fiber laser fabrication method. Finally, its simulated characteristics were compared with the experimental results.

References

[1] E. Arnieri, L. Boccia, G. Amendola, and G. Di Massa, "A compact high gain antenna for small satellite applications," *IEEE Transactions on Antennas and Propagation*, vol. 55, no. 2, pp. 277–282, 2007.

[2] F. Qin, S. S. Gao, Q. Luo, C.-X. Mao, C. Gu, G. Wei, J. Xu, J. Li, C. Wu, K. Zheng *et al.*, "A simple low-cost shared-aperture dual-band dual-polarized high-gain antenna for synthetic aperture radars," *IEEE Transactions on Antennas and Propagation*, vol. 64, no. 7, pp. 2914–2922, 2016.

[3] D. Caratelli, R. Cicchetti, V. Cicchetti, and O. Testa, "A wideband high-gain circularly-polarized dielectric horn antenna equipped with lamé-axicon stacked-disk lens for remote sensing, air traffic control and satellite communications," *IEEE Access*, vol. 11, pp. 20 912–20 922, 2023.

[4] H. W. Ehrenspeck, *High-Gain UHF Backfire Antenna for Communications, Telemetry, and Radio Astronomy*. Air Force Cambridge Research Laboratories, Office of Aerospace Research ..., 1967, no. 129.

[5] W. Han, F. Yang, J. Ouyang, and P. Yang, "Low-cost wideband and high-gain slotted cavity antenna using high-order modes for millimeter-wave application," *IEEE Transactions on Antennas and Propagation*, vol. 63, no. 11, pp. 4624–4631, 2015.

[6] H. Wheeler, "Simple relations derived fom a phased-array antenna made of an infinite current sheet," *IEEE Transactions on Antennas and Propagation*, vol. 13, no. 4, pp. 506–514, 1965.

[7] A. U. Zaman and P.-S. Kildal, "Wide-band slot antenna arrays with single-layer corporate-feed network in ridge gap waveguide technology," *IEEE Transactions on antennas and propagation*, vol. 62, no. 6, pp. 2992–3001, 2014.

[8] C. Liu, S. Xiao, Y.-X. Guo, M.-C. Tang, Y.-Y. Bai, and B.-Z. Wang, "Circularly polarized beam-steering antenna array with butler matrix network," *IEEE Antennas and Wireless Propagation Letters*, vol. 10, pp. 1278–1281, 2011.

[9] A. A. Oliner, D. R. Jackson, and J. Volakis, "Leaky-wave antennas," *Antenna engineering handbook*, vol. 4, p. 12, 2007.

[10] M. Garcia-Vigueras, J. L. Gomez-Tornero, G. Goussetis, A. R. Weily, and Y. J. Guo, "1D-leaky wave antenna employing parallel-plate waveguide loaded with PRS and HIS," *IEEE Transactions on Antennas and Propagation*, vol. 59, no. 10, pp. 3687–3694, 2011.

[11] F. Costa, D. Bianchi, A. Monorchio, and G. Manara, "Linear Fabry-Perot/leaky-wave antennas excited by multiple sources," *IEEE Transactions on Antennas and Propagation*, vol. 66, no. 10, pp. 5150–5159, 2018.

[12] N. Wang, L. Talbi, Q. Zeng, and J. Xu, "Wideband Fabry-Perot resonator antenna with electrically thin dielectric superstrates," *IEEE Access*, vol. 6, pp. 14 966–14 973, 2018.

[13] Z.-C. Ge, W.-X. Zhang, Z.-G. Liu, and Y.-Y. Gu, "Broadband and high-gain printed antennas constructed from Fabry–Perot resonator structure using EBG or FSS cover," *Microwave and Optical Technology Letters*, vol. 48, no. 7, pp. 1272–1274, 2006.

[14] N. Wang, Q. Liu, C. Wu, L. Talbi, Q. Zeng, and J. Xu, "Wideband Fabry-Perot resonator antenna with two complementary FSS layers," *IEEE Transactions on Antennas and Propagation*, vol. 62, no. 5, pp. 2463–2471, 2014.

[15] M. W. Niaz, Y. Yin, R. A. Bhatti, Y.-M. Cai, and J. Chen, "Wideband Fabry-Perot resonator antenna employing multilayer partially reflective surface," *IEEE Transactions on Antennas and Propagation*, vol. 69, no. 4, pp. 2404–2409, 2020.

[16] A. Hosseini, F. De Flaviis, and F. Capolino, "A 60 GHz simple-to-fabricate single-layer planar Fabry-Perot cavity antenna," *IET Microwaves, Antennas & Propagation*, vol. 9, no. 4, pp. 313–318, 2015.

[17] R. M. H. Bilal, M. Borgese, S. Genovesi, G. Manara, and F. Costa, "High directional Fabry-Perot millimeter-wave antenna for D-band spectrum," pp. 1–4, 2024.

[18] M. Hajj, E. Rodes, D. Serhal, T. Monédière, B. Jecko *et al.*, "Design of sectoral antennas using a metallic EBG structure and multiple sources feeding for base station applications," *International Journal of Antennas and Propagation*, vol. 2008, p. 6, 2008.